Front. Chem. Sci. Eng. 2021, 15(1): 35–48
https://doi.org/10.1007/s11705-020-1937-6

REVIEW ARTICLE

Recent progress on nanostructure-based broadband absorbers and their solar energy thermal utilization

Tong Zhang (✉)[1,2,3], Shan-Jiang Wang[1,3], Xiao-Yang Zhang[1,2,3], Ming Fu[1], Yi Yang[1], Wen Chen[1], Dan Su[2,3]

1 Joint International Research Laboratory of Information Display and Visualization, School of Electronic Science and Engineering, Southeast University, Nanjing 210096, China

2 Key Laboratory of Micro-Inertial Instrument and Advanced Navigation Technology, Ministry of Education, School of Instrument Science and Engineering, Southeast University, Nanjing 210096, China

3 Suzhou Key Laboratory of Metal Nano-Optoelectronic Technology, Suzhou Research Institute of Southeast University, Suzhou 215123, China

Abstract Nanostructure-based broadband absorbers are prominently attractive in various research fields such as nanomaterials, nanofabrication, nanophotonics and energy utilization. A highly efficient light absorption in wider wavelength ranges makes such absorbers useful in many solar energy harvesting applications. In this review, we present recent advances of broadband absorbers which absorb light by nanostructures. We start from the mechanism and design strategies of broadband absorbers based on different materials such as carbon-based, plasmonic or dielectric materials and then reviewed recent progress of solar energy thermal utilization dependent on the superior photo-heat conversion capacity of broadband absorbers which may significantly influence the future development of solar energy utilization, seawater purification and photoelectronic device design.

Keywords nanostructured broadband absorbers, solar energy harvesting, thermal utilization

1 Introduction

Artificial absorbers cover a broadband electromagnetic (EM) wavelength range that includes perfect broadband absorbers, black absorbers or metamaterials based absorbers [1–3]. They have attracted significant attention in the research fields and projected to have immense applications in passive and active optical processing [4–6], chemical engineering [7,8], radar cloaking [9], biomedical therapy [10,11] and anti-microbial [12]. Much of the studies are devoted to the development of artificial absorbers having significant light absorption capability in broadband wavelength range using nanotechnologies, and primarily focused on the enhancement of the absorption of EM waves using nanostructure-based surfaces [13,14], functional multilayers [15–17], or liquid mixtures [18]. In recent years, investigations from the aspects of both the absorption mechanism and fabrication technologies in the nanostructure-based broadband absorbers make rapid progress, towards the fabrication of broadband absorbers with much higher performance, lower material and fabrication costs, as well as faster production [19–21]. Related to this, many new concepts of applications have also been proposed and demonstrated. Among these applications, solar energy harvesting and relative thermal unitization receive huge interests [22–25]. On the earth, solar irradiation covers the broadband wavelength range of E waves from 200 to 2500 nm, and even much wider in space contains enormous energy, which is clean and inexhaustible [26,27]. As such solar energy in broadband is absorbed, and the stored light can be converted into different types of energies for various applications, such as solar steam generation and seawater distillation [28–30], photocatalyst [31,32] and other emerging applications [33–35]. It is, therefore, becoming a highly prospective research direction and receives wider concern by both academia and public that whether and how this renewable energy can be utilized in a highly efficient way.

In this review, we mainly focused on two aspects mentioned above. The first one is related to recent progress on how to develop broadband absorbers that can absorb electromagnetic waves from visible to infrared wavelength ranges and even extending to longer wavelength range, followed by mechanistic studies, the design principles of new nanostructures, and related fabrication technologies. For comparison, nanostructured dielectrics such as carbon-based nanomaterials and metallic plasmonic materials are

Received January 9, 2020; accepted March 19, 2020

E-mail: tzhang@seu.edu.cn

also discussed. The second aspect is on the recent improvements of solar energy harvesting using structured broadband absorbers and their applications, which mainly focuses on the conversion efficiency between different forms of energies, stability and compatibility of materials in working environments. Besides, the future directions for the development of photothermal utilization based on broadband absorbers are considered.

2 Mechanism and fabrication of nanostructure-based broadband absorbers

The ideal perfect broadband absorbers have the capability of substantial optical absorption and near-zero reflectance capacity that covers a broadband wavelength range [36–38]. To meet such a requirement, different light absorption mechanisms based on various materials and structures have been studied. Among them, currently, carbon-based nanostructures [39], plasmonic nanostructures [40,41], dielectric nanostructures [42], and complexed structures having synergistic effects [36,43,44] are the main research directions. Table 1 lists the major parameters of different types of nanostructure-based broadband absorbers.

2.1 Carbon-based nanostructure

Carbon is a typical material with high optical absorption and high conversion of light-to-heat in the range of visible to mid-infrared, and combined with its intrinsic light-weight and low-cost, have been widely considered for its application in broadband absorbers. In order to enhance the light absorption and reduce the reflectance of carbon materials, many types of carbon-based nanostructures such as carbon black (CB) [45–47], carbon nanotube (CNT) [48,49], carbon aerogel [50–54], graphene [55–58] and other carbon containing composites [59–62] have been extensively studied for the construction of perfect absorbers. In recent years, many advancements in this area have been reported, as shown in Fig. 1.

CB, an easily obtained carbon nanostructure with random size distribution and large surface area, is widely studied for the development of broadband absorbers. Li et al. suggested a fabrication method for black absorber using CB-coated fabric [45], where CB was readily adsorbed on the microfibers in the fabric using the dip-coating method to obtain a broadband absorber with a high absorbance above 90% in the range from 300 to 2500 nm. The hydrophilic surface property of the substrate was also improved by CB. Owing to excellent rheological and homogeneous distribution properties, CB, together with graphene oxide (GO) could also be useful for the preparation of 3D printing ink, using the construction of super black evaporator with light absorption of ~99.0% in the broader wavelength range between 250 and 2500 nm [46].

CNTs are also well investigated for the development of absorbers with super low reflectance. To increase the light absorption in the layer of CNTs, the light path should be prolonged, and surface reflectance should be suppressed as much as possible. Nearly perfect absorbers with a very low reflectance of 0.045% were demonstrated using well-aligned CNT arrays with a thickness of 300 μm, which provided a light path long enough compared to their absorption length of light (several micrometers in the visible range) [48]. Meanwhile, because of their hollow

Table 1 Examples of different types of absorbers, range of wavelength, light absorption and photothermal conversion efficiencies.

Types of absorbers	Range of wavelength	Light absorption	Photothermal conversion efficiency	Ref.
CB/PVDF-HFP	300–2500 nm	> 90%	88.9% under 1 sun	[45]
CB/AAO	2.5–15.3 μm	~97.5%	not given	[47]
CNT/GO	200–1200 nm	> 97%	85.6% under 1 sun	[49]
Carbon aerogels	430–675 nm	> 99.8%	not given	[52]
CNT aerogels	250–2500 nm	~99%	86.8% under 1 sun	[54]
Paper-based GO/Silicone	250–2500 nm	visible > 90% infrared > 80%	89.7% under 1 sun	[56]
GO/wood	500–1100 nm	> 80%	83% under 12 sun	[57]
MIM structure with plasmonic meta-materials	300–2000 nm	91.3%	77.3% under 100 sun	[80]
MIM structure with 2D tungsten arrays	300–2000 nm	90%	not given but with 800 K thermal stability	[108]
Sputtered gold membrane	400–2500 nm	~91%	57% under 20 sun	[89]
Copper cauliflower	200–800 nm	~98%	> 60% under 1 sun	[79]
Porous *p*-PEGDA–PANi hydrogel	250–2500 nm	98.5%	91.5% under 1 sun	[105]
3D aluminium NPs/AAM	500–2500 nm	> 96%	88.4% under 4 sun and 91% under 6 sun	[19]
Gold NPs/AAO	0.4–10 μm	~99%	> 90% under 4 sun	[66]

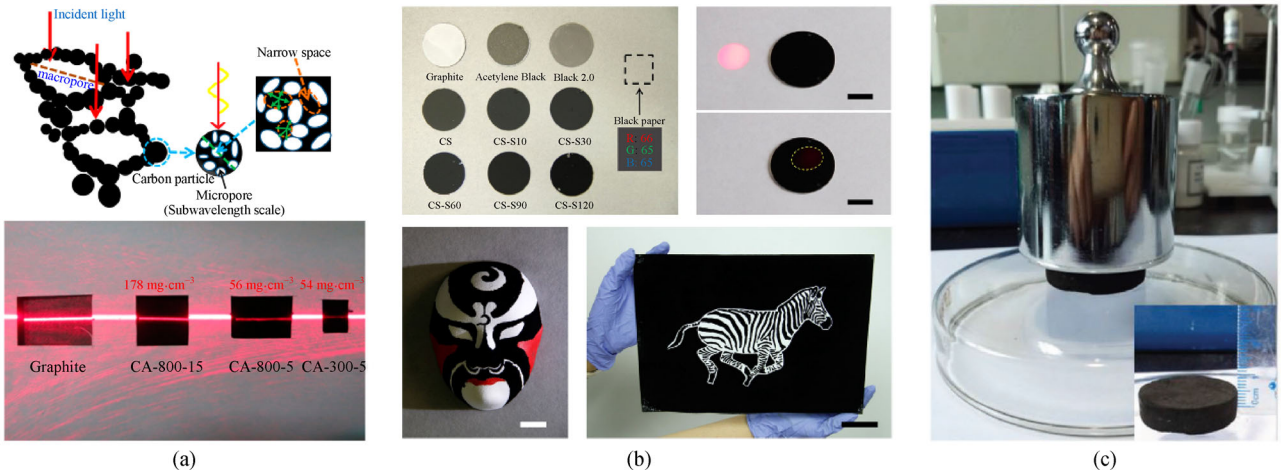

Fig. 1 (a) Abundant porous structures and super hydrophilic characteristics based on carbon aerogels. Reprinted with permission from Ref. [52]. Copyright 2016, American Chemical Society; (b) Super black coatings composed of carbonized polymeric porous spheres. Reprinted with permission from Ref. [61]. Copyright 2019, American Chemical Society; (c) 3D, porous and superwetting CNT aerogels. Reprinted with permission from Ref. [54]. Copyright 2019, Wiley-VCH.

structure, the effective index of CNTs is very close to 1, and therefore the surface reflectance is completely suppressed when incident light reaches the surface of the CNTs from the air.

However, the performance of the CNT array-based absorbers is highly dependent on the fabrication and large-scale equipment. To reduce the cost and processing difficulties, many studies focus on carbon aerogels and layered stacks of graphene. Microporous carbon aerogels composed of low-density carbon nanoparticles and nanochains [51–53] or nanotubes possessing the hierarchically nanoporous structure [54] have also shown excellent light absorption capacity in broadband, as shown in Fig. 1(c). For such aerogels with a high surface area and low-density carbon materials, the effective refractive index of the composite is highly dependent on the ratio between randomly distributed microporous structures of carbon. Light can be trapped and multi-reflect within the porous structures and eventually absorbed by carbon, as shown in Fig. 1(a). A reflectance of ~0.19% (within a material density of 0.01−0.02 $g \cdot cm^{-3}$) in the visible range using carbon nanoparticle aerogels [52], and less than 1% in the range of 200−2500 nm using CNT aerogels [54] have been reported recently. Because of their rich porous structures and super hydrophilic surfaces, such carbon aerogels are also considered to be good candidates for water transport, and solar steam generation, which have been discussed in the following section.

The two-dimensional and large surface area featured graphene has also been well investigated for the development of large scale super broadband absorbers [63,64]. Microchannel structures composed of GO, reduced graphene oxide (rGO) composite membranes, and hierarchical structure deposited by multilayer graphene with excellent light absorption capacity have been demonstrated by various relatively easy fabrication methods [56,57,60,62]. The above studies focused on the scalable production of perfect absorbers. Recently, Anguita et al. demonstrated that in nanoscale, the deposition of a few layers of graphene could significantly improve the broadband light absorption performance of optoelectronic devices [55]. They showed that by integrating multilayer graphene with a thickness of 15 nm attached on the surface of nanostructured Ti, the synergetic optical enhancement brought by metal nanostructures and stacked 2D graphene make such structures to have a superior ability of light absorption ($>99\%$ from UV to IR). Besides, it has been found that the optical absorption of carbon-based nanostructures could be further enhanced by defect-engineering [65].

2.2 Plasmonic nanostructure-based broadband absorbers

The plasmonic nanostructure is another potential candidate considered for the construction of broadband absorbers owing to the subwavelength light confinement property of the metal. Light can be confined and absorbed by nanostructured plasmonic materials such as Au, Ag, Cu and Al [19,66–68]. For elemental plasmonic nanostructures, for example, nanospheres, nanorods and nanoplates, their localized surface plasmon resonance (LSPR) bands (corresponding to the maximum interaction waveband between light and nanostructures) are usually narrow and located in the UV and visible ranges [67,69–72]. Compared to carbon-based absorbers, plasmonic nanostructures are easily acquired due to their controllable performance by quickly choosing the different shape, size, aggregation state, or modification forms (doping, alloying

and heterostructures) [69,72,73]. However, absorption capacities in the mid-infrared range and high-temperature resistance of them are essential for further exploration. To extend the utility of plasmonic absorber in a broader wavelength range, the followed strategies are shown in Fig. 2.

At first, the metal-insulator-metal (MIM) nanostructures are constructed, as shown in Fig. 2(a) [74]. It could be observed from the bottom to upper layers that such configuration typically contains a layer of metal, a thin layer of insulator, and a nanostructured metal layer on the top. Plasmonic top layer contains randomly or orderly distributed plasmonic nanostructures, and gratings or arrays can be fabricated by different techniques, such as self-assembly of chemically synthesized nanoparticles [74,75], sputter deposition of porous metal layer [76], transfer printing [77], laser writing [78,79] or standard top-down nanofabrication processes [80–82]. Light in the broadband can be confined by the following principles: (1) when light reaches on the surface of small metal nanostructures which have large absorption cross-section, the scattering behavior of light is suppressed and most of the light distributed in the LSPR band is absorbed by those plasmonic nanostructures and finally converted into heat; (2) LSPR band of dense aggregation of plasmonic nanostructures with gaps of a few nanometers becomes wider and shifts to the longer wavelength range; and (3) Fano resonance and multiple reflectances of light between the top and bottom metal layers localize more light which further increases the light absorption length. MIM structure based on Au nanoparticles with a size distribution around 5 nm demonstrates a wide absorption band with a reflectance of less than 10% in the range 400 to 750 nm [74]. However, the absorption decreased in the longer wavelength range, which is far away from the LSPR band of Au nanospheres or nanodisks [74,76,83].

To extend the absorption of MIM configuration, anisotropic plasmonic nanostructure arrays [75,84] or randomly distributed nanoworms [76,78] based top layers were studied, which shows a broader absorption band extending to over 1 μm. By tuning the topological surface of the plasmonic structures, the absorption band was further extended to a broader range [81,85−89]. An increase in the multiple periods of insulator-metal layers [90,91] also demonstrated to be an effective way to enhance the absorption further and extend the bandwidth of light. The broadband absorption principle of MIM configuration works well not only for thin-film devices but also is valid in the nanoscale. Ho et al. established Au film supported dumbbell Au/TiO_2 nanocavities with broader absorption in the visible region (500−900 nm), which was resulted from the synergetic effects of LSPR of Au nanorods and d-band transition of Au film [92].

Different from the MIM structures, plasmonic structures constructed by randomly distributed metal nanoplate aggregation [93], nanoflowers [79,94], nano-branches and nano-meshwork [95] can also confine broadband lights from visible to near-infrared ranges. The morphological features of such plasmonic structures are more complicated as compared to elemental nanostructures with uniform size and shape. Therefore, they have multiple LSPR bands and many hot spots, which are also highly

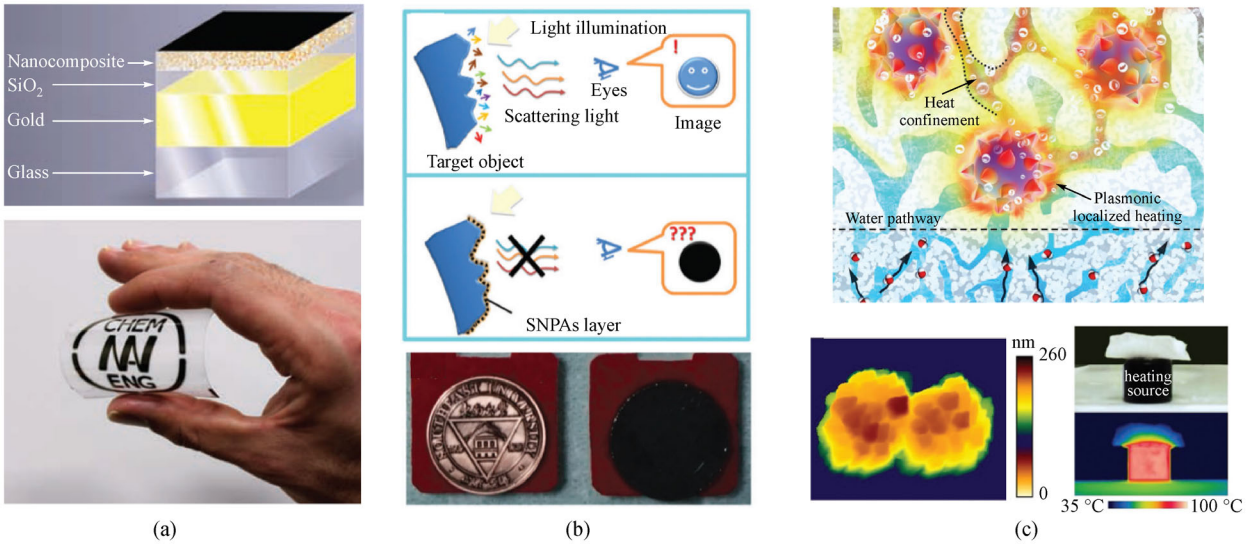

Fig. 2 (a) MIM structures based broadband absorbers. Reprinted with permission from Ref. [74]. Copyright 2011, Wiley-VCH; (b) Randomly distributed Ag nanoplates aggregation based absorbers. Reprinted with permission from Ref. [93]. Copyright 2018, the Royal Society of Chemistry; (c) Au nanostars embedded on silica gel for broadband absorption. Reprinted with permission from Ref. [97]. Copyright 2018, Wiley-VCH.

dependent on their complicated and anisotropic structures [93,95]. This could be the probable reason for their localization of light in a much broader wavelength range compared to smaller nanoparticles. Such randomly distributed nanostructures are easily obtained during the chemical synthesis of anisotropic nanostructures with a much higher density of chemicals than under conventional synthesis conditions. When the nucleation and crystal growth occur very fast during synthesis, it leads to aggregation or linked nanostructures, which appear as black color in the solutions [93,95]. Similarly, metal nanoframes [96] with mixed geometry parameters, nanostars [94,97] having multiple tips, nanospheres with rough surfaces [82], thin metal layers containing random pores [98] can also be used to construct broadband absorbers having excellent light confinement and photothermal conversion effect in a wider range. Apart from the above chemical synthesis method, other low-cost techniques have also been demonstrated, which are suitable for the fabrication of broadband absorbers. Piragash et al. demonstrated wet chemical etching as a practical approach to fabricate porous metasurfaces with a broadband absorption from 400 to 800 nm [99]. Fan et al. reported that disordered cauliflower-shaped hierarchical nanostructures on the copper surface with a rather broad range from 200 to 2000 nm could be fabricated using a one-step laser direct writing approach [79].

Other interesting strategies of plasmonic absorbers include the construction of various plasmonic nanostructures with different light confinement configurations and mechanisms [16,89,90]. The structured surface composed of multi-period anisotropic sawtooth arrays showed that it could effectively trap light covering the mid-infrared range (absorption $> 86\%$ in the range of 3−6 μm) [90]. In this configuration, the gradual effective indexes of the structured surface suppress backscattering. 'Slow-light' waveguide modes arising from the vertically stacked plasmonic condensers with different widths promoted the absorption of light with different wavelengths. It was also demonstrated that subwavelength plasmonic concentrators based on gap trapping effect existing on the adjacent surface plasmon polaritons waveguides could trap light in an extreme broadband range from 400 nm to 17 μm [89].

Besides, for optical absorption and photothermal applications which mainly depend on plasmonic induced hot-carrier generation, plasmonic materials possessing more optical absorption, are desirable. Compared to Au, titanium nitride has not only a relatively large negative ε_1, but also a larger positive ε_2 value. While titanium nitride also exhibits better thermal and chemical stabilities compared to conventionally used noble metals [100]. Studies have proved that such new types of plasmonic materials are suitable for the fabrication of highly-efficient broadband absorbers both in visible and infrared wavelength ranges [101−103].

2.3 Dielectric nanostructures-based broadband absorbers

Dielectric nanostructures with non-plasmonic properties were also considered as candidates for broadband absorbers [104–108]. One-dimensional and two-dimensional CuO and polymer nanowires with a high optical absorption coefficient also demonstrated excellent broadband light absorption capacity [104,105]. Dielectric metasurfaces composed of ordered TiO_2 nanofins showed absolute efficiency ($> 78\%$) in the visible range [106]. Light diffraction induced Rayleigh anomaly was existing in the tandem nanosized grating-based dielectric surface, which induced to higher absorption of ~90% from 300 nm to 2.0 μm [108]. Compared to metal-based materials, dielectric materials have better thermal and environmental stabilities which make them a very competitive candidate for broadband light trapping applications [20,108].

2.4 Synergistic effect in broadband absorbers

In practical applications, substantial optical absorption in different wavelength ranges is targeted. For the synergistic effect in combining with plasmonic nanostructures, carbon-based nanomaterials, together with dielectrics having high optical absorption, are considered in the design of super black absorbers [19,58,59,66,109–112]. Zhu et al. achieved high-efficiency absorption of solar energy ($> 99\%$, 0.4–10 μm) by designing 3D porous anodic aluminum oxide (AAO) templated Au nanoparticle structures [66]. The cooperative coupling effects of densely packed plasmonic Au nanoparticles and waveguide effects brought by a 3D porous AAO template, making it a superior candidate for the utilization of ultra-broadband of the solar spectrum. To further reduce the cost, they replaced Au nanoparticles to Al nanoparticles based on a similar mechanism and route and applied it into plasmon based seawater desalination devices at first [19]. Similarly, to further strengthen the intensity of light absorption and extend the absorption of solar spectrum, Song et al. accomplished adjustable EM wave absorption by growing vertically aligned ZnO nanowires on rGO foam, where they observed the stability and absorption of EM wave were improved as compared to pure rGO foam [58]. Wang et al. reported about a hybrid optical absorption structure with 92% light to heat conversion efficiency by combining plasmonic hollow and porous Au/Ag nanocubes with GO membrane. The localization of the optical field and coupling effects resulted from the plasmonic nanostructures further enhanced and extended the absorption of the solar spectrum [59]. Adding plasmonic particles to enhance the light absorption and conversion of light to heat was also indicated in other pioneering works. Wang et al. designed a multi-functional tandem heterojunction structure, including semiconductor nanosheets, plasmonic metals, and quantum dots. The synergistic effects of optical

absorption from these three materials and oriented electrical transportation paths have remarkably enhanced the photons trapping in the solar spectrum and utilization of light to heat [112]. Therefore, specifically in the target of obtaining the super-broadband light absorption, the synergistic effect with a hybrid system is deemed to be the optimized structures which utilize the features of per unit [113,114].

3 Applications of solar energy harvesting

The above discussion confirms that many strategies can realize broadband absorption of light covering the range of the solar spectrum. As solar energy in broadband can be effectively collected by the nanostructures and finally converted into heat, many new concepts towards practical applications for the thermal utilization of solar energy were proposed, which is progressing rapidly. In this section, the discussion is centered on the major applications from new concepts, including solar steam generation and desalination [28–31,115], photocatalytic reaction [40,116,117] and other photothermal applications [118–120] (Fig. 3).

3.1 Steam generation and seawater desalination

The significant conversion of light to heat formed by broadband absorbers makes them suitable for solar energy-driven steam generation and seawater desalination. These novel concepts meet urge demand for solving the shortage of freshwater in the globe. In these applications, the design of effective light absorbers and construction of special water transporting pathway are critical for enhancing the utilization of solar energy and reducing heat loss between desalination membrane and seawater. In this context, some of the crucial factors, including the design of absorbers, water transporting pathway, thermal stability, as well as other parameters for practical applications, are discussed below.

3.1.1 Management of heating and water transportation pathway

On this, several design strategies were reported [38,121–125]. One way is to fabricate multilayer membranes having multifunctional layers which can directly keep floating on water [38,126,127]. In these structures, the top layer is

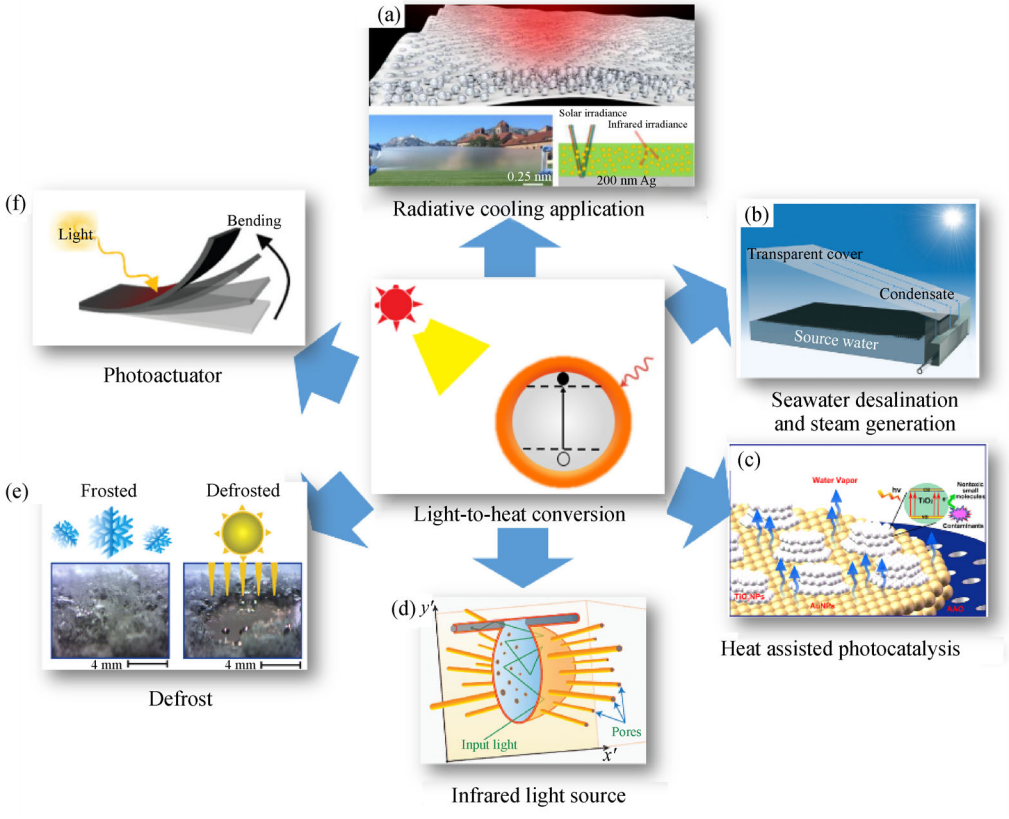

Fig. 3 Applications of nanostructured broadband absorbers. (a) Reprinted with permission from Ref. [118]. Copyright 2017, American Association for the Advancement of Science; (b) Reprinted with permission from Ref. [115]. Copyright 2018, the Royal Society of Chemistry; (c) Reprinted with permission from Ref. [116]. Copyright 2015, American Chemical Society; (d) Reprinted with permission from Ref. [120]. Copyright 2015, Springer Nature; (e) Reprinted with permission from Ref. [119]. Copyright 2018, American Chemical Society; (f) Reprinted with permission from Ref. [37]. Copyright 2018, the Royal Society of Chemistry.

used for the light absorption of broadband solar energy. The bottom layer is the thermal insulating layer, which prevents heat exchange from the bulk water underneath so that the heat is localized highly at the interface of air and liquid. In order to float on water, the thermal insulating layer is porous and loosely formed. The heat isolation mostly benefits its pores filled with air as well. The efficiency of heat collection of the floating membrane is improved to a great extent compared to that of a conventional absorber film which is placed at the bottom and heats the whole bulk water.

To utilize solar energy more adequately and promote a fast water-vapor cycle, various smart designs of three-dimensional water transporting pathway were presented [123–125]. Hu et al. proposed light-weight, honeycomb carbon-based aerogels by freeze-drying and found a very low thermal conductivity of ~0.05 $W \cdot m^{-1} \cdot K^{-1}$, the solar energy conversion efficiency of ~83%, and an evaporation rate of 1.622 $kg \cdot m^{-2} \cdot h^{-1}$ under one sun [123]. Li et al. reported a capillary force induced three-dimensional steam generation structure based on GO through vertical three-dimensional printing [124]. The water was transported linearly by one-dimensional GO pillars using capillary and then converted to vapor by two-dimensional carbon-based broadband absorbers. Such a structure showed an energy conversion efficiency of 87.5% and an evaporation rate of 1.27 $kg \cdot m^{-2} \cdot h^{-1}$ under one-sun. Xu et al. demonstrated a bio-inspired solar steam system based on naturally grown mushrooms without any additional nano-fabrication process [125]. After carbonization, the fibrous stipe and umbrella-shaped surface of the mushroom served as water a pathway and evaporator, respectively. Simultaneously, nanosized porous structure in the mushroom became broadband absorbers with over 90% optical absorption from 250 to 2500 nm. This system showed an evaporation rate of 1.475 $kg \cdot m^{-2} \cdot h^{-1}$ and an energy conversion efficiency of 85% under one sun.

3.1.2 Thermal stability considerations

On account of broadband absorbers, which consist of plasmonic metal particles, the composition with gold is much stable than silver, although the absorption range of silver is much longer and tunable [21,66]. Compared to gold and silver, aluminum is an emerging material for the replacement owing to its high thermal stability and lower cost [19]. Spherical nanoparticles, especially with smaller size, are relatively stable during photothermal heating, but they showed weak absorption in infrared wavelength range. The anisotropic silver aggregations showed better absorption in the infrared wavelength range. However, they are less stable when heated up to a specific temperature as high as 70 °C as shown in Fig. 4 [93], and thus the absorption of longer wavelength is gradually reduced for long-term use. To overcome this problem, it is also feasible to modify inert materials to broadband absorbers in order to keep the original optical properties. The inert silicon dioxide was used as a protecting layer to prevent oxidation and melting of silver clusters in the high-temperature seawater desalination process [126]. Also, to avoid direct contact with heat, the anisotropic Au nanostars were protected by silica gel [97]. In the same way, aerogel-protected carbon-based broadband absorbers offered a similar feature due to their prominent intrinsic thermal stability.

Other inexpensive and refractory metal materials such as W, Bi, Ti and Ta are also considered in this field [80,108,128]. For example, Han et al. showed anisotropic $W/SiO_2/W$ nanohole arrays with 90% optical absorption in the range from 0.3 to 2.0 μm, which were working stable at

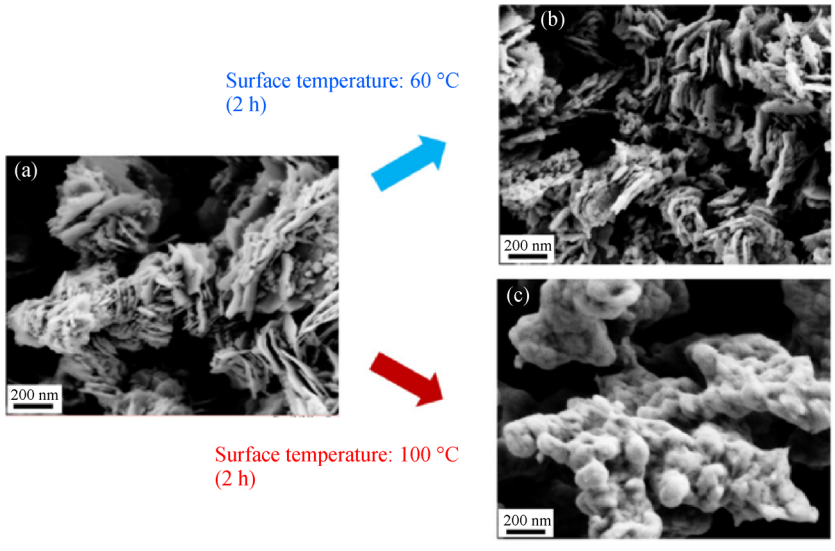

Fig. 4 Experimental investigations of thermal stability of silver nanostructures at different temperatures. Reprinted with permission from Ref. [93]. Copyright 2018, the Royal Society of Chemistry.

800 K [108]. Li et al. showed broadband absorbers consisting of Ti/Al_2O_3/Ta nanodisk arrays, which were functioning stably at 1000 K under the irradiation of 100 suns [80].

3.1.3 Other aspects of the solar steam generation

Besides, other aspects influencing the solar steam generation were also reported [129–131]. Dongare et al. pointed out that the rate of steam generation was influenced by the intensity of illumination nonlinearly [129]. In the process of evaporation, the intensity of vapor saturation pressure was exponentially dependent on the surface temperature, which played a key rule in increasing the rates of steam generation. Therefore, in achieving optimized strategies, a specific illumination intensity is required for a specific system.

When water-soluble broadband absorbers are used in the applications of solar steam generation, preventing secondary pollution becomes the focus [130,131]. Shi et al. demonstrated magnetic Fe_3O_4 modified broadband absorbers based on carbon, which was separated from the liquid easily by the externally applied magnetic force [130].

3.2 Applications in photocatalytic reactions

Broadband absorbers could also play an important role in enhancing the absorption of solar energy and local-heating generators, which lead to the acceleration of photocatalytic reactions, such as synthesis [132] or photodegradation [133] of organic compounds and solar water splitting [134,135]. Xiao et al. reported an enhanced plasmonic photocatalytic strategy using broadband absorbers [136]. In this reaction, the light was irradiated into the semiconductor-metal nanoparticle-based heterostructures and excited hot carriers, which eventually contributed to photocatalysis. When a layer of Au was added, the Au mirror layer, semiconductor and metal nanoparticles formed a plasmonic near-perfect absorber with the light absorption of ~94%, which was 5 folds higher compared to the photocatalytic structure with no mirror. Comparative experiments showed that this light absorption enhancement led to 29 folds increase in the solar energy conversion efficiency during the photocatalytic reaction. Mo et al. demonstrated that titanium nitride nanoparticle decorated TiO_2 showed significant enhancement in the solar energy conversion efficiency for solar water splitting [65]. In this strategy, plasmonic titanium nitride nanoparticle with the properties of higher light absorption and subwavelength light confinement over a wide wavelength range from 500 to 1200 nm significantly promoted the solar energy harvesting. Furthermore, the hot carrier transport and collection efficiency of titanium nitride and TiO_2 heterostructure were higher than Au and TiO_2 heterostructure [137]. Liu et al. demonstrated a bifunctional membrane with an optimized configuration for the local photothermal heating and water transport functions [116]. Based on the excellent thermal heating property of the embedded plasmonic broadband absorbers, such membranes could be used to both generate solar vapor and simultaneously promote photocatalytic degradation of organic dyes.

3.3 Other photothermal applications

Due to the excellent wider solar energy collection and light-to-heat conversion properties, broadband absorbers were also employed for various novel applications in case of consuming electronic devices [119,138–141], photoelectronic devices [142], and solar energy storage [37,143].

3.3.1 Deice and defrost

In recent years, it has been reported that broadband absorbers with superior photothermal effects are deemed to be promising for icephobicity and defrost, which meet practical applications and hence given intense attention. Mitridis et al. reported an ultrathin coating of Au nanoparticles, which absorbed a part of visible light uniformly for transparent window icephobicity, as shown in Fig. 5(a) [119]. To keep it transparent, the balance between transparency and light absorption was optimized by controlling the thickness and density of the Au nanoparticle layer. With the optimized light absorption of 37%, the transmitted colour was displayed well, and ice on the surface was defrosted within 80 s under the illumination of 2.4 suns at −16 °C. Dash et al. showed superhydrophobic anti-icing surfaces based on black absorbers with excellent photothermal trap performance (Fig. 5(b)) [140]. This is a reflective surface containing broadband absorbers that absorbed solar energy and achieved defrost immediately in several minutes. The temperature of such a surface was raised from −5 °C to 30 °C within 200 s in the open air, which demonstrated their reliability for practical applications.

3.3.2 Thermal actuators

Another emerging application is the photothermal induced self-folding effect, which has been applied in thermal actuators. In such a device, heaters made up of broadband absorbers, and the heat-responsive shape-memory polymer is integrated smartly. The features of fast response and trace detection, as well as remote light manipulation, resulted from such a smart design demonstrate potential in high-risk applications, such as in the detection of dangerous gases. Because of the properties of local photothermal heating, these broadband absorbers have widely used for applications related to assembly automation [141].

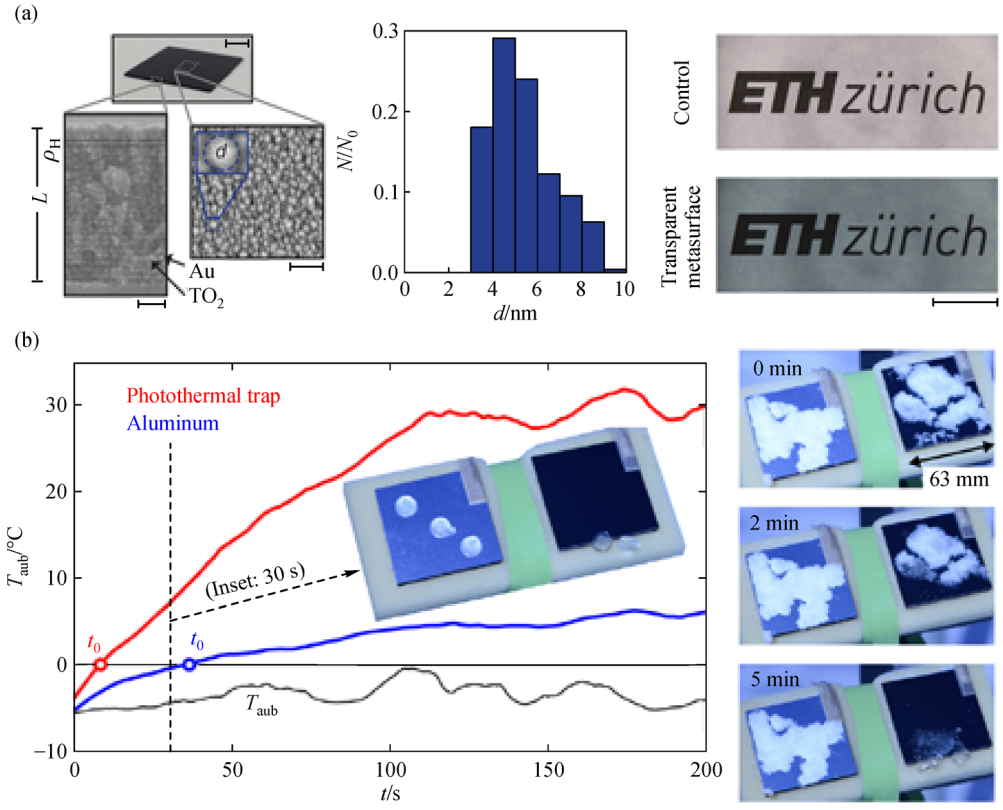

Fig. 5 (a) Transmission-type icephobicity and defrost based on transparent broadband absorbers. Reprinted with permission from Ref. [119]. Copyright 2018, American Chemical Society; (b) Superhydrophobic anti-icing surfaces based on the reflective type. Reprinted with permission from Ref. [140]. Copyright 2018, American Association for the Advancement of Science.

3.3.3 Thermal emitter and solar energy storage

In addition, such super black absorbers can be applied to photoelectronic devices. For example, Barho et al. utilized the structured broadband absorber for the development of thermal emitter infrared light source in detecting the infrared spectrum, which was highly cost-efficient compared to commercially available infrared light source [142]. The broadband light absorbers can also be applied for energy storage due to their capability converting of light-to-heat. For such an application, plasmons were mixed in the polymer to optimize thermal conductivity in order to improve the performance of solar-thermal harvesting [37].

4 Conclusions and perspectives

Nanostructure-based broadband absorbers have received the attention of researchers worldwide owing to their superior optical absorption, efficient light-to-heat conversion, and reliability in practical applications compared to conventional heat collection routes. However, several challenges need to be considered and worked out. Firstly, the physical mechanism of the process of light-to-heat conversion must be revealed in-depth, for example, it is still unclear about the dominant contribution of heat in the case of plasmonic-based broadband absorbers, and also both the hot carriers effects and photothermal effects need to be distinguished quantitatively. More efforts are also required in the field of energy utilization, such as high-efficiency solar energy driving electric power generation. Nanostructured broadband absorbers may be a prospective tool to greatly improve the sun energy utilization in broadband wave range and decrease the covering area of the concentrator system of a solar power station. However, to meet such requirement, ultra-high temperature steam with hundreds or even over one thousand centigrade is a pressing need [143,144], this means that receivers with high thermal stability are suitable for such application. Therefore, the development of nanostructured absorbers with thermal stability over hundreds of centigrade could be a very attractive research direction. With regard to other emerging research fields. For example, the photoelectric devices which convert photothermal effects into electricity, mechanics and acoustics, etc. A series of novel concepts combined with such effects could be proposed, which opens and extend the application areas in order to benefit of

society. Besides, the optimization of nanostructures based on low-cost, high stability, and eco-friendly are also necessary for large-scale fabrication and application.

Acknowledgements This work is supported by Ministry of Science and Technology of the People's Republic of China under Grant Number 2017YFA0205800, the National Natural Science Foundation of China (Grant Nos. 61875241, 11734005) and the Fundamental Research Funds for the Central Universities, Southeast University (Grant Nos. 2242018k1G020, 2242019k1G034).

References

1. Landy N I, Sajuyigbe S, Mock J J, Smith D R, Padilla W J. Perfect metamaterial absorber. Physical Review Letters, 2008, 100(20): 207402
2. Chen H T. Interference theory of metamaterial perfect absorbers. Optics Express, 2012, 20(7): 7165–7172
3. Ra'di Y, Simovski C R, Tretyakov S A. Thin perfect absorbers for electromagnetic waves: theory, design and realizations. Physical Review Applied, 2015, 3(3): 037001
4. Hajian H, Ghobadi A, Butun B, Ozbay E. Active metamaterial nearly perfect light absorbers: a review. Journal of the Optical Society of America. B, Optical Physics, 2019, 36(8): F131–F143
5. Yang X, Sun Z, Low T, Hu H, Guo X D, García de Abajo F J, Avouris P, Dai Q. Nanomaterial-based plasmon-enhanced infrared spectroscopy. Advanced Materials, 2018, 30(20): 1704896
6. Zhai Y, Chen G, Ji J, Ma X, Wu Z, Li Y, Wang Q. Large-scale, broadband absorber based on three-dimensional aluminum nanospike arrays substrate for surface plasmon induced hot electrons photodetection. Nanotechnology, 2019, 30(37): 375201
7. Zhu L, Gao M, Peh C K N, Ho G W. Solar-driven photothermal nanostructured materials designs and prerequisites for evaporation and catalysis applications. Materials Horizons, 2018, 5(3): 323–343
8. Yang M Q, Gao M, Hong M, Ho G W. Visible-to-NIR photon harvesting: progressive engineering of catalysts for solar-powered environmental purification and fuel production. Advanced Materials, 2018, 30(47): 1802894
9. Rhee J Y, Yoo Y J, Kim K W, Kim Y J, Lee Y P. Metamaterial-based perfect absorbers. Journal of Electromagnetic Waves and Applications, 2014, 28(13): 1541–1580
10. Liu Y, Bhattarai P, Dai Z, Chen X. Photothermal therapy and photoacoustic imaging via nanotheranostics in fighting cancer. Chemical Society Reviews, 2019, 48(7): 2053–2108
11. Jaque D, Martínez Maestro L, del Rosal B, Haro-Gonzalez P, Benayas A, Plaza J L, Martín Rodríguez E, García Solé J. Nanoparticles for photothermal therapies. Nanoscale, 2014, 6(16): 9494–9530
12. Baranwal A, Srivastava A, Kumar P, Bajpai V K, Maurya P K, Chandra P. Prospects of nanostructure materials and their composites as antimicrobial agents. Frontiers in Microbiology, 2018, 9: 422
13. Aydin K, Ferry V E, Briggs R M, Atwater H A. Broadband polarization-independent resonant light absorption using ultrathin plasmonic super absorbers. Nature Communications, 2011, 2(1): 517
14. Ng C, Cadusch J J, Dligatch S, Roberts A, Davis T J, Mulvaney P, Gómez D E. Hot carrier extraction with plasmonic broadband absorbers. ACS Nano, 2016, 10(4): 4704–4711
15. Lu G, Wu F, Zheng M, Chen C, Zhou X, Diao C, Liu F, Du G, Xue C, Jiang H, Chen H. Perfect optical absorbers in a wide range of incidence by photonic heterostructures containing layered hyperbolic metamaterials. Optics Express, 2019, 27(4): 5326–5336
16. Azad A K, Kort-Kamp W J M, Sykora M, Weisse-Bernstein N R, Luk T S, Taylor A J, Dalvit D A R, Chen H T. Metasurface broadband solar absorber. Scientific Reports, 2016, 6(1): 20347
17. Li X, Huang H, Bin H, Peng Z, Zhu C, Xue L, Zhang Z G, Zhang O Z, Ade H, Li Y. Synthesis and photovoltaic properties of a series of narrow bandgap organic semiconductor acceptors with their absorption edge reaching 900 nm. Chemistry of Materials, 2017, 29(23): 10130–10138
18. Hogan N J, Urban A S, Ayala-Orozco C, Pimpinelli A, Nordlander P, Halas N J. Nanoparticles heat through light localization. Nano Letters, 2014, 14(8): 4640–4645
19. Zhou L, Tan Y, Wang J, Xu W, Yuan Y, Cai W, Zhu S, Zhu J. 3D self-assembly of aluminium nanoparticles for plasmon-enhanced solar desalination. Nature Photonics, 2016, 10(6): 393–398
20. Ghobadi A, Hajian H, Gokbayrak M, Butun B, Ozbay E. Bismuth-based metamaterials: from narrowband reflective color filter to extremely broadband near perfect absorber. Nanophotonics, 2019, 8(5): 823–832
21. Zhu M, Li Y, Chen F, Zhu X, Dai J, Li Y, Yang Z, Yan X, Song J, Wang Y, Hitz E, Luo W, Lu M, Yang B, Hu L. Plasmonic wood for high-efficiency solar steam generation. Advanced Energy Materials, 2018, 8(4): 1701028
22. Khodasevych I E, Wang L, Mitchell A, Rosengarten G. Micro-and nanostructured surfaces for selective solar absorption. Advanced Optical Materials, 2015, 3(7): 852–881
23. Buller S, Strunk J. Nanostructure in energy conversion. Journal of Energy Chemistry, 2016, 25(2): 171–190
24. Zhang N, Han C, Fu X, Xu Y J. Function-oriented engineering of metal-based nanohybrids for photoredox catalysis: exerting plasmonic effect and beyond. Chem, 2018, 4(8): 1832–1861
25. Wang S J, Su D, Zhang T. Research progress of surface plasmons mediated photothermal effects. Acta Physica Sinica, 2019, 68(14): 144401
26. Thuillier G, Hersé M, Labs D, Foujols T, Peetermans W, Gillotay D, Simon P C, Mandel H. The solar spectral irradiance from 200 to 2400 nm as measured by the SOLSPEC spectrometer from the ATLAS and EURECA missions. Solar Physics, 2003, 214(1): 1–22
27. Thuillier G, Hersé M, Simon P C, Labs D, Mandel H, Gillotay D, Petermans W. The absolute solar spectral irradiance from 200 to 2500nm as measured by the SOLSPEC spectrometer with the ATLAS and EURECA missions. Physics and Chemistry of the Earth. Part C: Solar-terrestrial and Planetary Science, 2000, 25(5-6): 375–377
28. Deng Z, Zhou J, Miao L, Liu C, Peng Y, Sun L, Tanemura S. The emergence of solar thermal utilization: solar-driven steam generation. Journal of Materials Chemistry. A, Materials for Energy and Sustainability, 2017, 5(17): 7691–7709

29. Dao V D, Choi H S. Carbon-based sunlight absorbers in solar-driven steam generation devices. Global Challenges, 2018, 2(2): 1700094
30. Wang P. Emerging investigator series: the rise of nano-enabled photothermal materials for water evaporation and clean water production by sunlight. Environmental Science. Nano, 2018, 5(5): 1078–1089
31. Wang X, Wang F, Sang Y, Liu H. Full-spectrum solar-light-activated photocatalysts for light-chemical energy conversion. Advanced Energy Materials, 2017, 7(23): 1700473
32. Zhang T, Wang S J, Zhang X Y, Su D, Yang Y, Wu J Y, Xu Y Y, Zhao N. Progress in the utilization efficiency improvement of hot carriers in plasmon-mediated heterostructure photocatalysis. Applied Sciences (Basel, Switzerland), 2019, 9(10): 2093
33. Li W, Valentine J G. Harvesting the loss: surface plasmon-based hot electron photodetection. Nanophotonics, 2017, 6(1): 177–191
34. Ji C, Lee K T, Xu T, Zhou J, Park H J, Guo L J. Engineering light at the nanoscale: structural color filters and broadband perfect absorbers. Advanced Optical Materials, 2017, 5(20): 1700368
35. Baranov D G, Xiao Y, Nechepurenko I A, Krasnok A, Alù A, Kats M A. Nanophotonic engineering of far-field thermal emitters. Nature Materials, 2019, 18(9): 920–930
36. Yu P, Besteiro L V, Huang Y, Wu J, Fu L, Tan H H, Jagadish C, Wiederrecht G P, Govorov A O, Wang Z. Broadband metamaterial absorbers. Advanced Optical Materials, 2019, 7(3): 1800995
37. Kim J U, Lee S, Kang S J, Kim T. Materials and design of nanostructured broadband light absorbers for advanced light-to-heat conversion. Nanoscale, 2018, 10(46): 21555–21574
38. Gao M, Zhu L, Peh C K, Ho J W. Solar absorber material and system designs for photothermal water vaporization towards clean water and energy production. Energy & Environmental Science, 2019, 12(3): 841–864
39. Wang Y, Xu N, Li D, Zhu J. Thermal properties of two dimensional layered materials. Advanced Functional Materials, 2017, 27(19): 1604134
40. Long R, Li Y, Song L, Xiong Y. Coupling solar energy into reactions: materials design for surface plasmon-mediated catalysis. Small, 2015, 11(32): 3873–3889
41. Cushing S K, Wu N. Progress and perspectives of plasmon-enhanced solar energy conversion. Journal of Physical Chemistry Letters, 2016, 7(4): 666–675
42. Sharma G, Thakur B, Naushad M, Kumar A, Stadler F J, Alfadul S M, Mola G T. Applications of nanocomposite hydrogels for biomedical engineering and environmental protection. Environmental Chemistry Letters, 2018, 16(1): 113–146
43. Fan R H, Xiong B, Peng R W, Wang M. Constructing metastructures with broadband electromagnetic functionality. Advanced Materials, 2019, DOI: http://doi.org/10.1002/adma.201904646
44. Ghobadi A, Hajian H, Butun B, Ozbay E. Strong interference in planar, multilayer perfect absorbers: achieving high-operational performances in visible and near-infrared regimes. IEEE Nanotechnology Magazine, 2019, 13(4): 1–16
45. Li Y, Jin X, Zheng Y, Li W, Zheng F, Wang W, Lin T, Zhu Z. Tunable water delivery in carbon-coated fabrics for high efficiency solar vapor generation. ACS Applied Materials & Interfaces, 2019, 11(50): 46938–46946
46. Liu Z, Song H, Ji D, Li C, Cheney A, Liu Y, Zhang N, Zeng X, Chen B, Gao J, et al. Extremely cost-effective and efficient solar vapor generation under nonconcentrated illumination using thermally isolated black paper. Global Challenges, 2017, 1(2): 1600003
47. Li H, Wu L, Zhang H, Dai W, Hao J, Wu H, Ren F, Liu C. Self-assembly of carbon black/AAO templates on nanoporous Si for broadband infrared absorption. ACS Applied Materials & Interfaces, 2020, 12(3): 4081–4087
48. Yang Z P, Ci L, Bur J A, Lin S Y, Ajayan P M. Experimental observation of an extremely dark material made by a low-density nanotube array. Nano Letters, 2008, 8(2): 446–451
49. Li Y, Gao T, Yang Z, Chen C, Luo W, Song J, Hitz E, Jia C, Zhou Y, Liu B, Yang B, Hu L. 3D-printed, all-in-one evaporator for high-efficiency solar steam generation under 1 sun illumination. Advanced Materials, 2017, 29(26): 1700981
50. Lamy-Mendes A, Silva R F, Durães L. Advances in carbon nanostructure-silica aerogel composites: a review. Journal of Materials Chemistry. A, Materials for Energy and Sustainability, 2018, 6(4): 1340–1369
51. Yang F, Zhang Y, Yang X, Zhong M, Yi Z, Liu X, Kang X, Luo J, Li J, Wang C Y, et al. Enhanced photothermal effect in ultralow-density carbon aerogels with microporous structures for facile optical ignition applications. ACS Applied Materials & Interfaces, 2019, 11(7): 7250–7260
52. Sun W, Du A, Feng Y, Shen J, Huang S, Tang J, Zhou B. Super black material from low-density carbon aerogels with subwavelength structures. ACS Nano, 2016, 10(10): 9123–9128
53. Xie P, Sun W, Liu Y, Du A, Zhang Z, Wu G, Fan R. Carbon aerogels towards new candidates for double negative metamaterials of low density. Carbon, 2018, 129: 598–606
54. Mu P, Zhang Z, Bai W, He J, Sun H, Zhu Z, Liang W, Li A. Superwetting monolithic hollow-carbon-nanotubes aerogels with hierarchically nanoporous structure for efficient solar steam generation. Advanced Energy Materials, 2019, 9(1): 1802158
55. Anguita J V, Ahmad M, Haq S, Allam J P, Silva S R. Ultra-broadband light trapping using nanotextured decoupled graphene multilayers. Science Advances, 2016, 2(2): e1501238
56. Wang Z, Ye Q, Liang X, Xu J, Chang C, Song C, Shang W, Wu J, Tao P, Deng T. Paper-based membranes on silicone floaters for efficient and fast solar-driven interfacial evaporation under one sun. Journal of Materials Chemistry. A, Materials for Energy and Sustainability, 2017, 5(31): 16359–16368
57. Liu K K, Jiang Q, Tadepalli S, Raliya R, Biswas P, Naik R R, Singamaneni S. Wood-graphene oxide composite for highly efficient solar steam generation and desalination. ACS Applied Materials & Interfaces, 2017, 9(8): 7675–7681
58. Liu F, Wang L, Bradley R, Zhao B, Wu W. Highly efficient solar seawater desalination with environmentally friendly hierarchical porous carbons derived from halogen-containing polymers. RSC Advances, 2019, 9(50): 29414–29423
59. Liu F, Zhao B, Wu W, Yang H, Ning Y, Lai Y, Bradley R. Low cost, robust, environmentally friendly geopolymer-mesoporous carbon composites for efficient solar powered steam generation. Advanced Functional Materials, 2018, 28(47): 1803266

60. Guo J, Li D, Zhao H, Zou W, Yang Z, Qian Z, Yang S, Yang M, Zhao N, Xu J. Cast-and-use super black coating based on polymer-derived hierarchical porous carbon spheres. ACS Applied Materials & Interfaces, 2019, 11(17): 15945–15951
61. Guo J, Li D, Zhao H, Zou W, Yang Z, Qian Z, Yang S, Yang M, Zhao N, Xu J. Cast-and-use super black coating based on polymer-derived hierarchical porous carbon spheres. ACS Applied Materials & Interfaces, 2019, 11(17): 15945–15951
62. Wang L L, Zhu G, Wei Y, Zeng J, Yu X, Li Q, Xie H. Integrating nitrogen-doped graphitic carbon with Au nanoparticles for excellent solar energy absorption properties. Solar Energy Materials and Solar Cells, 2018, 184: 1–8
63. Liu F, Lai Y, Zhao B, Bradley R, Wu W. Photothermal materials for efficient solar powered steam generation. Frontiers of Chemical Science and Engineering, 2019, 13(4): 636–653
64. Bao Q, Loh K P. Graphene photonics, plasmonics and broadband optoelectronic devices. ACS Nano, 2012, 6(5): 3677–3694
65. Mo Z, Xu H, Chen Z, She X, Song Y, Wu J, Yan P, Xu L, Lei Y, Yuan S, Li H. Self-assembled synthesis of defect-engineered graphitic carbon nitride nanotubes for efficient conversion of solar energy. Applied Catalysis B: Environmental, 2018, 225: 154–161
66. Zhou L, Tan Y, Ji D, Zhu B, Zhang P, Xu J, Gan Q, Yu Z, Zhu J. Self-assembly of highly efficient, broadband plasmonic absorbers for solar steam generation. Science Advances, 2016, 2(4): e1501227
67. Zhang X Y, Xu J J, Wu J Y, Shan F, Ma X D, Chen Y Z, Zhang T. Seeds triggered massive synthesis and multi-step room temperature post-processing of silver nanoink-application for paper electronics. RSC Advances, 2017, 7(1): 8–19
68. Chan G H, Zhao J, Hicks E M, Schatz G C, Van Duyne R P. Plasmonic properties of copper nanoparticles fabricated by nanosphere lithography. Nano Letters, 2007, 7(7): 1947–1952
69. Zhang X Y, Zhou H L, Shan F, Xue X M, Su D, Liu Y R, Chen Y Z, Wu J Y, Zhang T. Synthesis of silver nanoplate based two-dimension plasmonic platform from 25 nm to 40 μm: growth mechanism and optical characteristic investigation *in situ*. RSC Advances, 2017, 7(88): 55680–55690
70. Sau T K, Murphy C J. Seeded high yield synthesis of short Au nanorods in aqueous solution. Langmuir, 2004, 20(15): 6414–6420
71. Zhou Y, Yu S H, Wang C Y, Li X G, Zhu Y R, Chen Z Y. A novel ultraviolet irradiation photoreduction technique for the preparation of single-crystal Ag nanorods and Ag dendrites. Advanced Materials, 1999, 11(10): 850–852
72. Zhang X Y, Hu A, Zhang T, Lei W, Xue X J, Zhou Y, Duley W W. Self-assembly of large-scale and ultrathin silver nanoplate films with tunable plasmon resonance properties. ACS Nano, 2011, 5 (11): 9082–9092
73. Brown A M, Sundararaman R, Narang P, Goddard W A III, Atwater H A. Nonradiative plasmon decay and hot carrier dynamics: effects of phonons, surfaces, and geometry. ACS Nano, 2016, 10(1): 957–966
74. Hedayati M K, Javaherirahim M, Mozooni B, Abdelaziz R, Tavassolizadeh A, Chakravadhanula V S K, Zaporojtchenko V, Strunkus T, Faupel F, Elbahri M. Design of a perfect black absorber at visible frequencies using plasmonic metamaterials. Advanced Materials, 2011, 23(45): 5410–5414
75. Zhang H, Guan C, Luo J, Yuan Y, Song N, Zhang Y, Fang J, Liu H. Facile film-nanooctahedron assembly route to plasmonic metamaterial absorbers at visible frequencies. ACS Applied Materials & Interfaces, 2019, 11(22): 20241–20248
76. Liu Z, Liu X, Huang S, Pan P, Chen J, Liu G, Gu G. Automatically acquired broadband plasmonic-metamaterial black absorber during the metallic film-formation. ACS Applied Materials & Interfaces, 2015, 7(8): 4962–4968
77. Meudt M, Jakob T, Polywka A, Stegers L, Kropp S, Runke S, Zang M, Clemens M, Görrn P. Plasmonic black metasurface by transfer printing. Advanced Materials Technologies, 2018, 3(11): 1800124
78. Berean K J, Sivan V, Khodasevych I, Boes A, Della Gaspera E, Field M R, Kalantar-Zadeh K, Mitchell A, Rosengarten G. Laser-induced dewetting for precise local generation of Au nanostructures for tunable solar absorption. Advanced Optical Materials, 2016, 4(8): 1247–1254
79. Fan P, Wu H, Zhong M, Zhang H, Bai B, Jin G. Large-scale cauliflower-shaped hierarchical copper nanostructures for efficient photothermal conversion. Nanoscale, 2016, 8(30): 14617–14624
80. Li Y, Li D, Zhou D, Chi C, Yang S, Huang B. Efficient, scalable, and high-temperature selective solar absorbers based on hybrid-strategy plasmonic metamaterials. Solar RRL, 2018, 2(8): 1800057
81. Yu W, Lu Y, Chen X, Xu H, Shao J, Chen X, Sun Y, Hao J, Dai N. Large-area, broadband, wide-angle plasmonic metasurface absorber for midwavelength infrared atmospheric transparency window. Advanced Optical Materials, 2019, 7(20): 1900841
82. Hao J, Wang J, Liu X, Padilla W J, Zhou L, Qiu M. High performance optical absorber based on a plasmonic metamaterial. Applied Physics Letters, 2010, 96(25): 251104
83. Hedayati M K, Faupel F, Elbahri M. Tunable broadband plasmonic perfect absorber at visible frequency. Applied Physics. A, Materials Science & Processing, 2012, 109(4): 769–773
84. Matsumori K, Fujimura R. Broadband light absorption of an Al semishell-MIM nanostrucure in the UV to near-infrared regions. Optics Letters, 2018, 43(12): 2981–2984
85. Liu X, Starr T, Starr A F, Padilla W J. Infrared spatial and frequency selective metamaterial with near-unity absorbance. Physical Review Letters, 2010, 104(20): 207403
86. Lu Y, Dong W, Chen Z, Pors A, Wang Z, Bozhevolnyi S I. Gap-plasmon based broadband absorbers for enhanced hot-electron and photocurrent generation. Scientific Reports, 2016, 6(1): 30650
87. Mulla B, Sabah C. Multiband metamaterial absorber design based on plasmonic resonances for solar energy harvesting. Plasmonics, 2016, 11(5): 1313–1321
88. Desiatov B, Goykhman I, Mazurski N, Shappir J, Khurgin J B, Levy U. Plasmonic enhanced silicon pyramids for internal photoemission Schottky detectors in the near-infrared regime. Optica, 2015, 2(4): 335–338
89. Bae K, Kang G, Cho S K, Park W, Kim K, Padilla W J. Flexible thin-film black gold membranes with ultrabroadband plasmonic nanofocusing for efficient solar vapour generation. Nature Communications, 2015, 6(1): 10103
90. Cui Y, Fung K H, Xu J, Ma H, Jin Y, He S, Fang N X. Ultrabroadband light absorption by a sawtooth anisotropic metamaterial slab. Nano Letters, 2012, 12(3): 1443–1447

91. Wu D, Liu C, Liu Y, Yu L, Yu Z, Chen L, Ma R, Ye H. Numerical study of an ultra-broadband near-perfect solar absorber in the visible and near-infrared region. Optics Letters, 2017, 42(3): 450–453
92. Ho K H W, Shang A, Shi F, Lo T W, Yeung P H, Yu Y S, Zhang X, Wong K, Lei D Y. Plasmonic Au/TiO_2-dumbbell-on-film nanocavities for high-efficiency hot-carrier generation and extraction. Advanced Functional Materials, 2018, 28(34): 1800383
93. Zhang X Y, Shan F, Zhou H L, Su D, Xue X M, Wu J Y, Chen Y Z, Zhao N, Zhang T. Silver nanoplate aggregation based multifunctional black metal absorbers for localization, photothermic harnessing enhancement and omnidirectional light antireflection. Journal of Materials Chemistry. C, Materials for Optical and Electronic Devices, 2018, 6(5): 989–999
94. Shan F, Zhang X Y, Fu X C, Zhang L J, Su D, Wang S J, Wu J Y, Zhang T. Investigation of simultaneously existed Raman scattering enhancement and inhibiting fluorescence using surface modified gold nanostars as SERS probes. Scientific Reports, 2017, 7(1): 6813
95. Zhang X Y, Zhang T, Zhu S Q, Wang L D, Liu X, Wang Q L, Song Y J. Fabrication and spectroscopic investigation of branched silver nanowires and nanomeshworks. Nanoscale Research Letters, 2012, 7(1): 596
96. Karampelas I H, Liu K, Alali F, Furlani E P. Plasmonic nanoframes for photothermal energy conversion. Journal of Physical Chemistry C, 2016, 120(13): 7256–7264
97. Gao M, Peh C K, Phan H T, Zhu L, Ho G W. Solar absorber gel: localized macro-nano heat channeling for efficient plasmonic Au nanoflowers photothermic vaporization and triboelectric generation. Advanced Energy Materials, 2018, 8(25): 1800711
98. Wang L D, Zhang T, Zhang X Y, Li R Z, Zhu S Q, Wang L N. Synthesis of ultra-thin gold nanosheets composed of steadily linked dense nanoparticle arrays using magnetron sputtering. Nanoscience and Nanotechnology Letters, 2013, 5(2): 257–260
99. Piragash R M K, Venkatesh A, Moorthy V H S. Wet-chemical etching: a novel nanofabrication route to prepare broadband random plasmonic metasurfaces. Plasmonics, 2019, 14(2): 365–374
100. Li M, Guler U, Li Y, Rea A, Tanyi E K, Kim Y, Noginov M A, Song Y, Boltasseva A, Shalaev V M, Kotov N A. Plasmonic biomimetic nanocomposite with spontaneous subwavelength structuring as broadband absorbers. ACS Energy Letters, 2018, 3 (7): 1578–1583
101. Chang C C, Nogan J, Yang Z P, Kort-Kamp W J M, Ross W, Luk T S, Dalvit D A R, Azad A K, Chen H T. Highly plasmonic titanium nitride by room-temperature sputtering. Scientific Reports, 2019, 9 (1): 15287
102. Nagarajan A, Vivek K, Shah M, Achanta V G, Gerini G. A broadband plasmonic metasurface superabsorber at optical frequencies: analytical design framework and demonstration. Advanced Optical Materials, 2018, 6(16): 1800253
103. Kharitonov A, Kharintsev S. Tunable optical materials for multiresonant plasmonics: from TiN to TiON. Optical Materials Express, 2020, 10(2): 513–531
104. Bhattacharjee A, Ahmaruzzaman M. CuO nanostructures: facile synthesis and applications for enhanced photodegradation of organic compounds and reduction of *p*-nitrophenol from aqueous phase. RSC Advances, 2016, 6(47): 41348–41363
105. Yin X, Zhang Y, Guo Q, Cai X, Xiao J, Ding Z, Yang J. Macroporous double-network hydrogel for high-efficiency solar steam generation under 1 sun illumination. ACS Applied Materials & Interfaces, 2018, 10(13): 10998–11007
106. Devlin R C, Khorasaninejad M, Chen W T, Oh J, Capasso F. Broadband high-efficiency dielectric metasurfaces for the visible spectrum. Proceedings of the National Academy of Sciences of the United States of America, 2016, 113(38): 10473–10478
107. Wang S, Chen F, Ji R, Hou M, Yi F, Zheng W, Zhang T, Lu W. Large-area low-cost dielectric perfect absorber by one-step sputtering. Advanced Optical Materials, 2019, 7(9): 1801596
108. Han S, Shin J H, Jung P H, Lee H, Lee B J. Broadband solar thermal absorber based on optical metamaterials for high-temperature applications. Advanced Optical Materials, 2016, 4 (8): 1265–1273
109. Gan Q, Bartoli F J, Kafafi Z H. Plasmonic-enhanced organic photovoltaics: breaking the 10% efficiency barrier. Advanced Materials, 2013, 25(17): 2385–2396
110. Song G, Yuan Y, Liu J, Liu Q, Zhang W, Fang J, Gu J, Ma D, Zhang D. Biomimetic superstructures assembled from Au nanostars and nanospheres for efficient solar evaporation. Advanced Sustainable Systems, 2019, 3(6): 1900003
111. Kiriarachchi H D, Awad F S, Hassan A A, Bobb J A, Lin A, El-Shall M S. Plasmonic chemically modified cotton nanocomposite fibers for efficient solar water desalination and wastewater treatment. Nanoscale, 2018, 10(39): 18531–18539
112. Wang K, Xing Z, Du M, Zhang S, Li Z, Pan K, Zhou W. Plasmon Ag and CdS quantum dot co-decorated 3D hierarchical ball-flower-like Bi_5O_7I nanosheets as tandem heterojunctions for enhanced photothermal-photocatalytic performance. Catalysis Science & Technology, 2019, 9(23): 6714–6722
113. Dong W, Qiu Y, Yang J, Simpson R E, Cao T. Wideband absorbers in the visible with ultrathin plasmonic-phase change material nanogratings. Journal of Physical Chemistry C, 2016, 120(23): 12713–12722
114. Wang M, Zhang J, Wang P, Li C, Xu X, Jin Y. Bifunctional plasmonic colloidosome/graphene oxide-based floating membranes for recyclable high-efficiency solar-driven clean water generation. Nano Research, 2018, 11(7): 3854–3863
115. Wang P. Emerging investigator series: The rise of nano-enabled photothermal materials for water evaporation and clean water production by sunlight. Environmental Science. Nano, 2018, 5(5): 1078–1089
116. Liu Y, Lou J, Ni M, Song C, Wu J, Dasgupta N P, Tao P, Shang W, Deng T. Bioinspired bifunctional membrane for efficient clean water generation. ACS Applied Materials & Interfaces, 2016, 8(1): 772–779
117. Yang X, Wang D. Photocatalysis: from fundamental principles to materials and applications. ACS Applied Energy Materials, 2018, 1 (12): 6657–6693
118. Zhai Y, Ma Y, David S N, Zhao D, Lou R, Tan G, Yang R, Yin X. Scalable-manufactured randomized glass-polymer hybrid metamaterial for daytime radiative cooling. Science, 2017, 355(6329): 1062–1066

119. Mitridis E, Schutzius T M, Sicher A, Hail C U, Eghlidi H, Poulikakos D. Metasurfaces leveraging solar energy for icephobicity. ACS Nano, 2018, 12(7): 7009–7017
120. Huang J, Liu C, Zhu Y, Masala S, Alarousu E, Han Y, Fratalocchi A. Harnessing structural darkness in the visible and infrared wavelengths for a new source of light. Nature Nanotechnology, 2016, 11(1): 60121
121. Ni G, Li G, Boriskina S V, Li H, Yang W, Zhang T J, Chen G. Steam generation under one sun enabled by a floating structure with thermal concentration. Nature Energy, 2016, 1(9): 16126
122. Li J, Du M, Lv G, Zhou L, Li X, Bertoluzzi L, Liu C, Zhu S, Zhu J. Interfacial solar steam generation enables fast-responsive, energy-efficient, and low-cost off-grid sterilization. Advanced Materials, 2018, 30(49): 1805159
123. Hu X, Xu W, Zhou L, Tan Y, Wang Y, Zhu S, Zhu J. Tailoring graphene oxide-based aerogels for efficient solar steam generation under one sun. Advanced Materials, 2017, 29(5): 1604031
124. Li Y, Gao T, Yang Z, Chen C, Kuang Y, Song J, Jia C, Hitz E M, Yang B, Hu L. Graphene oxide-based evaporator with one-dimensional water transport enabling high-efficiency solar desalination. Nano Energy, 2017, 41: 201–209
125. Xu N, Hu X, Xu W, Li X, Zhou L, Zhu S, Zhu J. Mushrooms as efficient solar steam-generation devices. Advanced Materials, 2017, 29(28): 1606762
126. Gao M, Connor P K N, Ho G W. Plasmonic photothermic directed broadband sunlight harnessing for seawater catalysis and desalination. Energy & Environmental Science, 2016, 9(10): 3151–3160
127. Wang X, He Y, Liu X, Cheng G, Zhu J. Solar steam generation through bio-inspired interface heating of broadband-absorbing plasmonic membranes. Applied Energy, 2017, 195: 414–425
128. Li Y, Lin C, Zhou D, An Y, Li D, Chi C, Huang H, Yang S, Tso C Y, Chao C Y H, Huang B. Scalable all-ceramic nanofilms as highly efficient and thermally stable selective solar absorbers. Nano Energy, 2019, 64: 103947
129. Dongare P D, Alabastri A, Neumann O, Nordlander P, Halas N J. Solar thermal desalination as a nonlinear optical process. Proceedings of the National Academy of Sciences of the United States of America, 2019, 116(27): 13182–13187
130. Shi L, He Y, Huang Y, Jiang B. Recyclable Fe_3O_4@ CNT nanoparticles for high-efficiency solar vapor generation. Energy Conversion and Management, 2017, 149: 401–408
131. Wang X, Ou G, Wang N, Wu H. Graphene-based recyclable photo-absorbers for high-efficiency seawater desalination. ACS Applied Materials & Interfaces, 2016, 8(14): 9194–9199
132. Lang X, Chen X, Zhao J. Heterogeneous visible light photocatalysis for selective organic transformations. Chemical Society Reviews, 2014, 43(1): 473–486
133. Aslam U, Rao V G, Chavez S, Linic S. Catalytic conversion of solar to chemical energy on plasmonic metal nanostructures. Nature Catalysis, 2018, 1(9): 656–665
134. Zheng Z, Xie W, Huang B, Dai Y. Plasmon-enhanced solar water splitting on metal-semiconductor photocatalysts. Chemistry (Weinheim an der Bergstrasse, Germany), 2018, 24(69): 18322–18333
135. Ghobadi T G U, Ghobadi A, Ozbay E, Karadas F. Strategies for plasmonic hot-electron-driven photoelectrochemical water splitting. ChemPhotoChem, 2018, 2(3): 161–182
136. Xiao Q, Connell T U, Cadusch J J, Roberts A, Chesman A S R, Gómez D E. Hot-carrier organic synthesis via the near-perfect absorption of light. ACS Catalysis, 2018, 8(11): 10331–10339
137. Naldoni A, Guler U, Wang Z, Marelli M, Malara F, Meng X, Besteiro L V, Govorov A O, Kildishev A V, Boltasseva A, Shalaev V M. Broadband hot-electron collection for solar water splitting with plasmonic titanium nitride. Advanced Optical Materials, 2017, 5(15): 1601031
138. Li X, Shang J, Wang Z. Intelligent materials: a review of applications in 4D printing. Assembly Automation, 2017, 37(2): 170–185
139. Kreder M J, Alvarenga J, Kim P, Aizenberg J. Design of anti-icing surfaces: smooth, textured or slippery? Nature Reviews. Materials, 2016, 1(1): 1–15
140. Dash S, de Ruiter J, Varanasi K K. Photothermal trap utilizing solar illumination for ice mitigation. Science Advances, 2018, 4(8): eaat0127
141. Yang Z, Han X, Lee H K, Phan-Quang G C, Koh C S L, Lay C L, Lee Y H, Miao Y E, Liu T, Phang I Y, Ling X Y. Shape-dependent thermo-plasmonic effect of nanoporous gold at the nanoscale for ultrasensitive heat-mediated remote actuation. Nanoscale, 2018, 10 (34): 16005–16012
142. Barho F B, Gonzalez-Posada F, Bomers M, Mezy A, Cerutti L, Taliercio T. Surface-enhanced thermal emission spectroscopy with perfect absorber metasurfaces. ACS Photonics, 2019, 6(6): 1506–1514
143. Chandrashekara M. Experimental analysis of high temperature solar selective coated box type receiver for desalination. International Journal of Ambient Energy, 2020, DOI: 10.1080/01430750.2020.1718752
144. Li Y, Choi S S, Yang C. Dish-Stirling solar power plants: Modeling, analysis, and control of receiver temperature. IEEE Transactions on Sustainable Energy, 2014, 5(2): 398–407